METEOSAT SECOND GENERATION (MSG)

J. Schmetz, P. Pili and S. Tjemkes
EUMETSAT
Darmstadt, Germany

Abstract: The paper presents the new generation of European geostationary meteorological satellites Meteosat Second Generation (MSG) which has capabilities greatly enhanced over the current Meteosat series: The twelve channel imager, called SEVIRI (Spinning Enhanced Visible and Infrared Imager) observes the full disk of the Earth with an unprecedented repeat cycle of 15 minutes. Pixels are sampled with a distance of 3 km and the high resolution visible channel even has 1 km sampling distance. Image data are digitised with 10 bits. Thermal IR channels have an onboard calibration and for the solar channels an operational vicarious procedure is developed aiming at an accuracy of 5%. Meteorological products are derived in so-called Satellite Application Facilities (SAF) and in the central Meteorological Product Extraction Facility (MPEF) at EUMETSAT in Darmstadt; those products are briefly introduced. A view toward future product enhancement and novel applications is given too. As additional scientific payload MSG carries a Geostationary Earth Radiation Budget (GERB) instrument. The first launch of MSG is scheduled for 2002.

1. INTRODUCTION

The meteorological community has benefited for more than two decades from the services of the current generation of Meteosat meteorological satellites, the first of which was launched in 1977. Meteosat image data are now an essential component of the Global Observing System and derived meteorological products are of great value to Numerical Weather Prediction (NWP), nowcasting and very short range forecasting (VSRF). For NWP application satellite tracked winds and more recently radiances are used in the analysis and data assimilation. The Meteosat Second Generation (MSG) system will significantly enhance the services and products that can be provided to the user community. As the current Meteosat, MSG is spin-stabilised. The MSG Programme covers a series of three identical satellites, MSG-1, -2 and -3, expected to provide observations and services over at least 12 years. MSG-1 is scheduled for launch in 2002 with MSG-2 to follow 18 months later. The MSG system is established under a cooperation between ESA and EUMETSAT. The Rutherford Appleton Laboratory (RAL), UK provides the Geostationary Earth Radiation Budget (GERB) instruments for flight on all three MSG satellites and associated data services. The following sections introduce MSG capabilities and products.

2. THE SEVIRI INSTRUMENT

The primary mission of MSG is the continuous observation of the Earth's full disk. This is achieved with the Spinning Enhanced Visible and Infrared Imager (SEVIRI) imaging radiometer. SEVIRI is a twelve channel imager observing the Earth-atmosphere system with a spatial sampling distance of 3 km in eleven channels. A high-resolution visible (HRV) channel covers half of the full disk with a 1 km spatial sampling. The actual field of view of the channels is about 4.8 km and 1.67 km.

2.1 Operating SEVIRI

A repeat cycle of 15 minutes for full-disk imaging provides unprecedented multi-spectral observations of rapidly changing phenomena (e.g. deep convection) and provides better and more numerous wind observations from the tracking of cloud features. Rapid scans of limited latitude belts are possible with shorter time intervals.

The imaging is performed by combining the satellite spin with the rotation (stepping) of the scan mirror. The images are taken from South to North and East to West. The E-W scan is achieved through the rotation of the satellite with a nominal spin rate of 100 revolutions per minute. The spin axis is nominally parallel to the North-South axis of the Earth. The scan from South to North is achieved through a scan mirror covering the Earth's disk with about 1250 scan lines; this provides 3750 image lines for channels 1 through 11 (see Table

1) since 3 detectors for each channel are used for the imaging. For the HRV (channel 12) 9 detectors sweep the Earth for one line scan. The number of line scans is programmable such that shorter repeat cycles can be performed. A full disk image is obtained within about 12 minutes (see Figure 1). This is followed by the calibration of the thermal IR channels with an on-board blackbody which is inserted into the optical path of the instrument (see section 2.4). Then the scan mirror returns to its initial scanning position.

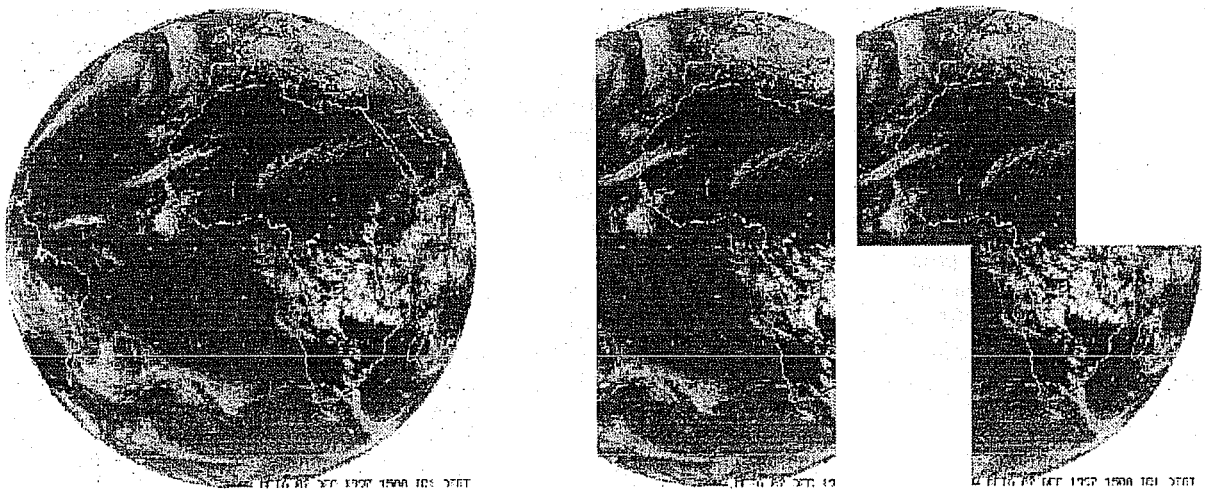

Figure 1: Coverage of MSG for repeat cycle of 15 minutes for channels 1 through 11 (ref. Table 1). The High resolution Visible (HRV), i.e. channel 12, covers only half the Earth in E-W, however the area of imaging can be selected.

2.1 SEVIRI Spectral Channels

Channel No.		Channel Spectral Band in μm		
		λ_{cen}	λ_{min}	λ_{max}
12	HRV	Broadband (silicon response)		
1	VIS0.6	0.635	0.56	0.71
2	VIS0.8	0.81	0.74	0.88
3	NIR1.6	1.64	1.50	1.78
4	IR3.9	3.90	3.48	4.36
5	WV6.2	6.25	5.35	7.15
6	WV7.3	7.35	6.85	7.85
7	IR8.7	8.70	8.30	9.1
8	IR9.7	9.66	9.38	9.94
9	IR10.8	10.80	9.80	11.80
10	IR12.0	12.00	11.00	13.00
11	IR13.4	13.40	12.40	14.40

Table 1: Spectral channel characteristics of SEVIRI providing central, minimum and maximum wavelength of the channels.

Most SEVIRI spectral channels build upon the heritage from other satellites which has the great advantage that the operational user community can readily use existing know-how to utilise SEVIRI radiance observations. Figure 2 shows the weighting functions of the thermal IR channels at 3.9, 6.2, 7.3, 8.7, 9.7, 10.8 ,12.0 and 13.4 μm. The heritage of channels can be summarised as follows:

VIS0.6 and VIS0.8: Known from the Advanced Very High Resolution Radiometer (AVHRR) of the polar orbiting NOAA satellites. They are essential for cloud detection, cloud tracking, scene identification, aerosol and land surface and vegetation monitoring.

NIR1.6: Discriminates between snow and cloud, ice and water clouds, and provides aerosol information. Observations are available from the Along Track Scanning Radiometer (ATSR) on ERS.
IR3.9: Known from AVHRR. Primarily for low cloud and fog detection (Eyre et.al., 1984). Also supports measurement of land and sea surface temperature at night. For MSG, the spectral band has been broadened to higher wavelengths to improve signal-to-noise ratio.
IR6.2 and IR7.3: Continues mission of Meteosat broadband water vapour channel for observing water vapour and winds. Enhanced to two channels peaking at different levels in the troposphere (see Figure 1). Also support height allocation of semitransparent clouds.
IR8.7: Known from the High resolution Infra Red Sounder (HIRS) instrument on the polar orbiting NOAA satellites. The channel provides quantitative information on thin cirrus clouds and supports the discrimination between ice and water clouds.
IR9.7: Known from HIRS and current GOES satellites. Ozone radiances could be used as an input to Numerical Weather Prediction (NWP). As an experimental channel, it will be used for tracking of ozone patterns that should be representative for wind motion in the lower stratosphere. The evolution of the total ozone field with time can also be monitored.
IR10.8 and IR12.0: Well-known split window channels (e.g. AVHRR). Essential to measure sea- and land-surface and cloud top temperatures.
IR13.4: CO_2 absorption channel known from former GOES VAS instrument. It improves height allocation of tenuous cirrus clouds (Menzel et al., 1983). In cloud free areas, it will provide temperature information from the lower troposphere that can be used for static instability (see GII product).

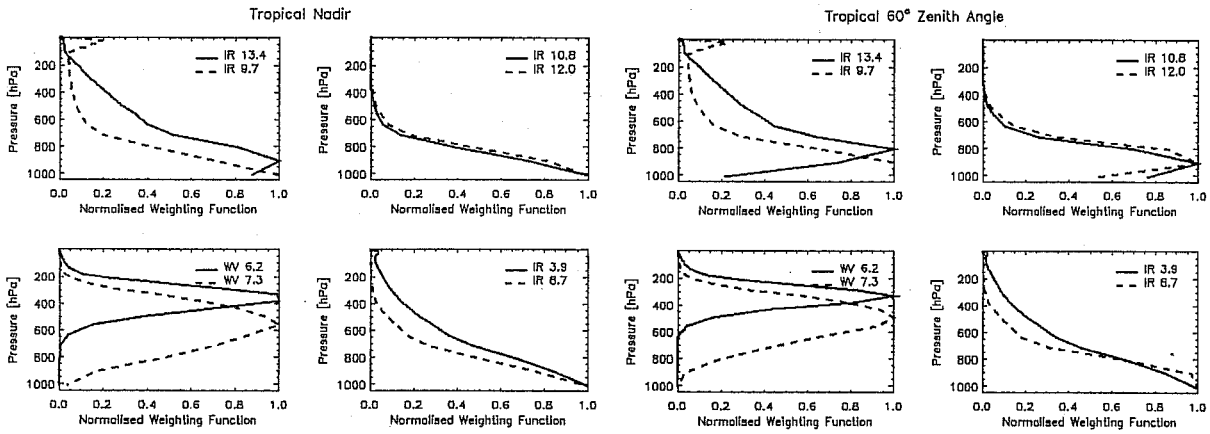

Figure 2: Weighting functions for the thermal IR channels of SEVIRI on MSG-1. The left four panels correspond to a tropical standard atmosphere and nadir view; the four panels to the right are for a viewing angle of 60°.

2.2 Radiometric Performance

The radiometric requirements for SEVIRI specify: i) short term error or noise, ii) mid-term drift error, and iii) bias or long-term drift error.
The short term error or noise requirement includes all factors affecting the radiometry during one nominal repeat cycle (15 minutes duration) and applies to in-orbit conditions at End Of Life (EOL). These are essentially: random noise, stability of temperature of detectors, crosstalk and straylight, stability of gain. Table 2 provides the measured performance of SEVIRI on MSG-1 and the specified requirements. Measured performance is based on tests complemented by a prediction of in-flight performances. Except for channel NIR1.6, the predicted in-orbit radiometric performances at EOL are better than the requirements. Thus excellent radiometric image quality can be expected.
The mid-term drift requirement limits the variation of the mean radiometric error in a sequence of nominal images. The requirement for the warm channels is a maximum drift over 1 day (i.e. 96 nominal repeat cycles) of less than 0.1% of the maximum of the dynamic range. The requirement for the cold (i.e. the thermal IR with cooled detectors) channels is a maximum drift between two on-board calibrations of less than 0.05K (or 0.1K for WV6.2 and WV7.3) at the maximum temperature of the dynamic range. The ground tests have shown that the worst case applies to channel IR12.0 requiring an on- board calibration every 10

images. It should, however, be noted that the baseline design of SEVIRI enables to perform one calibration per image cycle.

Channel	Short term radiometric error performances	Short term radiometric error requirements
HRV	0.93 at 1.3 W/(m² sr μm)	1.07 at 1.3 W/(m² sr μm)
VIS0.6	0.37 at 5.3 W/(m² sr μm)	0.53 at 5.3 W/ (m² sr μm)
VIS0.8	0.37 at 3.6 W/(m² sr μm)	0.49 at 3.6 W/(m² sr μm)
NIR1.6	0.25 at 0.75W/(m² sr μm)	0.25 at 0.75 W/(m² sr μm)
IR3.9	0.24K at 300K	0.35K at 300K
WV6.2	0.40K at 250K	0.75K at 250K
WV7.3	0.48K at 250K	0.75K at 250K
IR8.7	0.17K at 300K	0.28K at 300K
IR9.7	0.24K at 255K	1.5K at 255K
IR10.8	0.15K at 300K	0.25K at 300K
IR12.0	0.22K at 300K	0.37K at 300K
IR13.4	0.30K at 270K	1.80K at 270K

Table 2: Noise equivalent radiances and temperatures for the channels of the SEVIRI instrument on MSG-1 compared with the requirements. Values for the thermal IR channels refer to a focal plane temperature of 95K.

The bias and long-term drift requirement specifies the absolute radiometric error (i.e. the difference between the measured radiance and the actual radiance at the input of the instrument). Tests confirmed that the performance for all thermal IR channels is about 0.5 K for typical warm scene temperatures of 300 to 335 K (see also following section on calibration).

2.3 SEVIRI Calibration

The thermal IR channels of SEVIRI are calibrated with an on-board blackbody (Pili, 2000). The relationship between digital counts and the observed radiance is assumed to be linear:

$$C(L) = g\,L(\lambda, T) + C_0$$

Where C(L) is the digital count output from SEVIRI, $L(\lambda, T)$ the measured radiance, λ the wavelength (in practice a spectral interval), T the effective blackbody temperature of an observed scene (or the blackbody temperature), g the gain (or calibration coefficient) and C_0 the offset. The assumption of a linear relationship between counts and radiance is valid since small non-linearity are corrected for on ground before applying the linear calibration procedure.
SEVIRI uses the deep space as cold source and an internal blackbody as warm source for the calibration. While the deep space view is be obtained by viewing through the complete optical path of the instrument the blackbody is moved into the optical path avoiding the front optics. This design necessitates a correction to be applied to the blackbody calibration considering the optical properties of the front optics, whose characteristics have been measured before launch and whose temperature is monitored continuously. The blackbody can also be heated to allow for the determination of the correction factor. Overall a calibration performance better of about 0.5 K is expected for all thermal IR channels (Pili, 2000).

The solar channels (channels 1 –3 and 12) do not have an on-board calibration but have to rely on a vicarious method based on radiance observations over well-characterised targets (clear-sky desert, clear-sky ocean and optically thick high level clouds) and radiative transfer simulations (Govaerts et al., 2000). This new method of solar channel calibration will achieve an accuracy of the about 5% after the first year of operations as the characterisation of targets improves and quality control parameters will become better tuned.

3. MSG PRODUCTS

The derivation of level 2.0 meteorological products, is performed within the Applications Ground Segment (AGS) which consists of:
1) a Meteorological Products Extraction Facility (MPEF)
2) a network of satellite Application Facilities (SAF) located at National Weather Services and other institutions of EUMETSAT member states.

3.1 MPEF PRODUCTS

The Scenes Analysis (SCE) is the first step and an intermediate product of the MSG MPEF which is further used in the derivation of other products requiring either cloudy or clear pixels. The results of Scenes Analysis algorithm will provide per pixel and repeat cycle:
i) Identification of cloudy and clear pixels and a cloud mask, ii) Identification of scene type for each pixel, iii) Radiances at the top of the atmosphere.
The Scenes Analysis algorithm is based on threshold techniques (e.g. Saunders and Kriebel, 1988).
Advantage is taken of the 15 minute repeat cycle by using results of the previous image as first guess in the current image. SCE and Cloud Analysis are described in more detail by Lutz (1999).

Cloud Analysis (CLA) is based on the Scenes Analysis results and provides on a scale of 100 km x 100 km (or better) information about cloud cover, cloud top temperature, cloud top pressure/height and cloud type and phase. An important objective of the Cloud analysis product is to support the generation of the Atmospheric Motion Vectors (AMV). Therefore an intermediate product for each pixel and repeat cycle, which provides the necessary internal input to the Atmospheric Motion Vectors, is derived, but not disseminated. This intermediate (pixel scale) Cloud Analysis is also used for the Cloud Top Height product. It also provides input to the statistical information contained in the off-line Climate Data Sets product.
Cloud Top Height (CTH) is a derived product image, which provides the height of the highest cloud at a super-pixel resolution of 3x3 pixels. This product is for use in aviation meteorology. It provides the heights with a vertical resolution of 300 meter. Additionally the CTH product provides information about fog in the CTH processing segment.
Clear Sky Radiance (CSR) gives mean radiances (in Wm^{-2} sr^{-1} (cm^{-1}) $^{-1}$) for cloud-free pixels. Operational NWP centres will use CSR products from the MSG infrared channels in their analyses. The benefit will emerge with the advent of 4-d variational data assimilation systems that have the capability to utilise the frequent time observations from geostationary orbit (e.g. Munro et al., 1998).

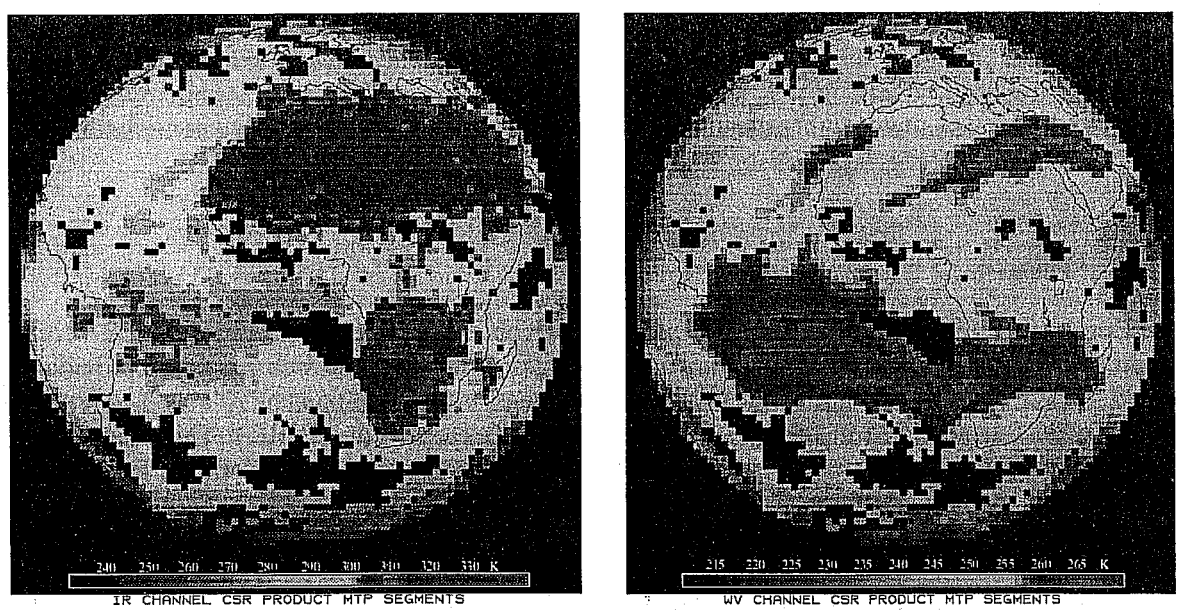

Figure 3: Clear-sky IR window radiance (left panel) and clear-sky water vapour radiance products. Results are from the MSG prototype algorithm applied to Meteosat-7.

Tropospheric Humidity (TH) provides estimates of layer-mean relative humidity for two tropospheric layers. One layer humidity (between about 600 and 200 hPa) is based on 6.3 μm clear sky radiances; this product is also known as UTH (upper tropospheric humidity) from the current Meteosat MPEF. The mean relative humidity of a second layer (between 850 and 300 hPa) uses clear sky 7.3 μm and is named MTH (mid-tropospheric humidity). The algorithm follows the improved UTH retrieval presented in Schmetz et al. (1995).

Atmospheric Motion Vectors (AMV) are the most important product for numerical weather prediction. The tropospheric AMVs will be derived from cloud and water vapour motion using primarily the 0.6 or 0.8 μm channel, the 10.8 μm channel and the 6.2 and 7.3 μm channels, respectively. The capabilities to extract lower stratospheric displacements vectors from ozone will also be exploited.

The product is based on conceptually validated ideas and methods (e.g. Schmetz at al., 1993 and Holmlund, 2000). An important feature, already implemented in the current Meteosat products, is the improved automatic quality control using quality indicators (Holmlund, 1998). The MSG algorithm also features novel concepts, such as i) a wind vector assignment to the exact target position, ii) improved target selection and enhancement, iii) improved quality control which benefits from the fact that wind fields from a single repeat cycle are used to derive a spatially dense final AMV product, iv) improved height assignment for semitransparent cloud tracers.

ISCCP Data Set (IDS) continues the support to the International Satellite Cloud Climatology Programme (ISCCP) providing three different data formats.

High Resolution Precipitation Index (HPI) continues the support to the Global Precipitation Climatology Project (GPCP) and provides the frequency of pixels for classes of brightness temperatures. Since it is indicative of convective (tropical) rainfall the product is confined to the latitudes between 40°S and 40°N.

Climate Data Set (CDS) provides statistical information about the scene classes in a processed segment (nominally 32x32 pixels). It is a concise summary of the radiances observed in a segment and potentially very useful for climatological studies of cloud and radiation fields.

Global Instability Index (GII) is an air mass parameter indicating the stability of the atmosphere at a scale of about 30 km. It is closely related to products from the SAF for Nowcasting and Very Short Range Forecasting, except that the GII is derived globally and disseminated. Based on successful applications and experience by NOAA/NESDIS with GOES lifted index products (Menzel et al., 1998) the idea for the GII emerged. Two algorithms are currently foreseen for the GII product i) a physical retrieval (Ma et al., 1999) and ii) an artificial neural network which has a lower performance overall but is computationally more efficient.

Total Ozone Product (TOZ) uses the 9.7 μm channel, other SEVIRI channels and correlative data and is derived with a regression algorithm (Orsolini and Karcher, 2000). The ozone observations are useful input for monitoring and forecasting UV radiation at the ground level. Preliminary studies have also shown that ozone observations at high temporal and spatial resolution may provide useful information about the winds in the upper troposphere and lower stratosphere (e.g. Riishojgaard, 1996). Alternatively, the ozone observations can be assimilated into a dynamical model with a suitable multivariate data assimilation system in which the forecast includes a prognostic equation for ozone.

3.2 SAF Products

This section provides a brief summary of SAF products which are based on MSG observations. More details on the products from SAFs are given on relevant web pages. Links to these web pages are provided via the EUMETSAT web page www.eumetsat.de under 'Programmes under development'. Table 3 provides the list of MSG products as specified in the End User Requirements Document (EURD). This includes products from the Ocean and Sea Ice SAF, the Ozone SAF and the MPEF. A more comprehensive list of agreed and targeted products can be summarised as follows:

- Examples of products from the Ocean and Sea Ice SAF include i) Atlantic Sea Surface Temperature, ii) Surface radiative fluxes over the Atlantic, iii) Sea Ice (Polar Atlantic): ice edge/cover, thickness/age.
- Examples of products from the Climate SAF are i) Sea Surface Temperature and sea ice cover, ii) Cloud parameters, iii) Surface radiation budget components, iv) Radiation budget components at TOA, v) humidity products.

- Examples of targeted products from the Land Analysis SAF are i) Vegetation parameters and biophysical indicators, ii) Snow cover, iii) Land Surface Temperature, emissivity and moisture, iv) Short wave and long wave radiation parameters.

This list is exemplary and may undergo further changes. Some of these products are composite and based on multi-mission data including MSG data as one source. Beyond this coarse cross-section of MSG-relevant SAF products, the interested reader is referred to the relevant SAF web pages to obtain more information on SAF products (see above). It is also noted that the SAF on Nowcasting and Very Short Range Forecasting develops software for a suite of products that can be derived from MSG. The software will be made available for local implementation.

3.3 Development Toward Day-2 Products

The improvement of Day-1 products, i.e. products available after commissioning, will be a continuous task. Future research and expected feedback on products from users will encourage those developments and should make it a necessity. Experience with operational satellite data processing systems has shown the usefulness of a continuous development and research that steadily pushes the utility of the satellite data.
Several improvements are already being planned. For instance, for the MPEF the Scenes Analysis and Atmospheric Motion Vectors (AMVs) can be enhanced. Tjemkes and Watts (2000) report on a research study which investigates new ways to perform a scenes analysis. The new method uses 'optimum estimation' Rodgers (1976) as novel way to infer simultaneously a set of cloud parameters and possibly surface features. This Enhanced Cloud Product (ECP) derives the following cloud micro-physical properties from SEVIRI observations: Optical Thickness, Mean Particle Radius, Cloud Top Temperature, Cloud Top Pressure, and Cloud Phase.

Another area for improvement are the Atmospheric Motion Vectors where two products will complement the current Day-1 baseline products:
i) Ozone Motion Vectors describe the displacement of total ozone features and include a height assignment of the derived vectors. In the baseline of the MSG-MPEF the use of total ozone product derived from observations in the IR 9.6 channel for the derivation of displacement vectors in the stratosphere was not foreseen. A study by Meteo France (part of the Ozone SAF) in collaboration with Dutch Weather Service (KNMI) has shown that the retrieved total ozone product retrieved from GOES-9 observations has distinct features on a synoptic scale, which could potentially be used to derive Ozone Motion Vectors. A limited pilot study by the EUMETSAT using the standard software to derive AMV further supports this.
ii) Low Level Winds over Land and Ocean will be an enhancement of the current low-level wind products. It describes the displacement of low level clouds derived from HRVIS, 0.6, 0.8 and 3.9 μm observations. In the baseline set-up of the MSG-MPEF the derivation of Atmospheric Motion Vectors over land is performed with the standard tracking software. However, the particular characteristics of low-level clouds over land (their spatial scale and life-time) and the complexity of the background (different types of vegetation, temperature gradients, other surface features) make the tracking of these clouds problematic. Currently the utilisation of those AMVs in NWP is very limited since NWP centers are not currently assimilating the low-level AMVs over land. In order to improve the quality of the low level wind field over land a new target selection, image enhancement, and cloud height and tracking procedures are developed that utilise the full capabilities of the SEVIRI instrument. Initial study results are encouraging (Szantai et al., 2000).

MSG will also provide new potential for observing components of the hydrological cycle which undergo rapid changes. Convective cloud processes related to thunderstorms or frontal systems require an appropriate monitoring with a high temporal repeat cycle. In particular cloud glaciation and precipitation formation occur rapidly and imagery from current geostationary satellites at the 30 minute time scale seem to be inadequate for capturing the transient processes that influence precipitation formation. The change in time of cloud microphysical state as observable from multispectral imagery may provide useful information on the formation of precipitation. Recent work by Rosenfeld and Lensky (2000) shows that the microphysical and precipitation forming processes can be observed with multispectral satellite imagery. Their work also demonstrates that transformations in the cloud microphysics due to biomass burning smoke and air pollution can be observed.

Product	Characteristics	Method	Coverage area	Product Frequency	Resolution (at SSP)	Method of distribution
Atmospheric Motion Vectors (AMV)	Wind vectors with heights assigned derived from cloudy and cloud-free segments; with quality indicators	Evolution of MTP-MPEF method	MSG processing area	1 h	100 km HRV: 30 km	GTS
Calibration Support (CAL)	Calibration information update using external ground truth data	Forward radiation modelling for all SEVIRI channels	N/A (refers to SEVIRI instrument)	15 min	N/A	In-house delivery to MSG Image Processing and MARF
Clear Sky Radiance (CSR)	Radiance values for clear sky and cleared sky segments	Evolution of method currently developed within the MTP, based on the MSG MPEF scenes analysis method	MSG processing area	1 h	100 km	GTS
Climate Data Set (CDS)	Results from Scenes Analysis, for continuity with MIEC and MTP MPEF product	Dataset based on Scenes Analysis results	MSG processing area	1 h	100 km	MARF retrieval
Cloud Analysis (CLA)	List of cloud layers with coverage, temperature, pressure per layer, cloud type and cloud phase	based on the MSG MPEF scenes analysis method	MSG processing area	3 h	100 km	GTS MSG HRIT/LRIT (imagery product)
Cloud Top Height (CTH)	Imagery product with cloud top height in steps of 300 metres	Evolution of MTP MPEF CTH product	MSG processing area	3 h	3x3 pixels	MSG HRIT/LRIT
High Resolution Precipitation Index (HPI)	Precipitation Index product for GPCP	GPCP Algorithm. Assignment of IR pixel to temperature classes according to the EBBT.	± 40 degrees of latitude ± 50 deg. of longitude	3h	1 ° by 1 ° grid	off-line delivery to GPCP centre
ISCCP Data Set (IDS)	Reduced resolution image sectors	Resampling of level 1.5 image data	MSG processing area	as defined by ISCCP	as defined by ISCCP	off-line delivery to ISCCP centre
Tropospheric Humidity (TH)	Upper and medium tropospheric relative humidity (in %)	Evolution of method used in MTP MPEF	MSG processing area	1 h	100 km; 2 layers	GTS
Total Ozone (TOZ)	total column density of ozone derived from MSG	Physical retrieval	MSG processing area	1 h	100 km	GTS
Global Instability Index (GII)	Air mass instability on synoptic scale	Method developed in external study (univ. Bonn) and SAF Nowcasting and VSRF	MSG processing area	1 h	30 km (TBC)	GTS MSG HRIT/LRIT
Atlantic Surface Radiative Fluxes (ASRF)	Surface solar and longwave downward and net fluxes	SW radiation from VIS data; LW from satellite cloud classification and NWP model outputs	Atlantic Ocean and adjacent seas	3 h	10 x 10 km	GTS Research networks
Atlantic Sea Surface Temperature (ASST)	Composite SST field at mesoscale spatial resolution	Multi-window techniques with a simple surface skin to bulk temperature transformation	Atlantic Ocean and adjacent seas	3 h	10 x 10 km	GTS Research networks
Clear-sky UV fields	UV distribution for clear-sky areas	Ozone forecast and Radiative Transfer calculations	Regional and Global [TBC]	at least once per day [TBC]	100 km	TBD

Table 3: Meteorological Products from MSG (from MSG End-User Requirements Document EUM/MSG/SPE/013 Issue 2.2)
Note that ASRF, ASST are products from the Ocean and Sea Ice SAF and Clear-Sky UV Field is developed by the Ozone SAF.

Generally speaking the 15 min repeat cycle of MSG for a full disk imaging is an excellent and unprecedented starting point for the observation of 'fast components' of the hydrological cycle (e.g.convection). It matches the typical observation cycle of meteorological weather radars. It remains to be seen whether more frequent imagery may be needed to push the current frontier of our understanding of the life cycle of deep convective clouds.

The utility of rapid scans from geostationary satellites for the derivation of winds and for nowcasting application has also been demonstrated by various researchers, mainly in the US and in Japan (for a review see Schmetz et al., 2000). Recently Europe has also made substantial efforts to utilise the potential of rapid scans; this was largely triggered by requests for rapid scans with Meteosat-6 in support of the Mesoscale Alpine Programme (MAP) in 1999 (Levizzani et al., 1998). Rosci et al. (2000) use the more frequent image repeat cycle to improve the detection of convective phenomena. Szantai et al. (2000) show that cloud motion winds over land are more numerous when the imaging frequency is reduced from 30 to 15 minutes. A reduction to 7.5 minutes provides another, though smaller, gain. Generally it appears that the advantage of rapid scans for the derivation winds from short-lived clouds would justify the scheduling of rapid scans (e.g. Velden et al., 2000). Again MSG provides unprecedented opportunities in those areas.

MSG also provides novel perspectives for applications over land (see EUMETSAT-SAI Report, 1999) because of its multispectral imagery in the visible, near-infrared and thermal infrared bands. The quantitative application of the visible and near-infrared bands will be facilitated through the development of an accurate operational vicarious calibration (Govaerts, 2000a). An interesting application is the monitoring of the land surface reflectance. The utility of such a product has been demonstrated by Pinty et al. (2000a and b) who derive a Meteosat surface albedo (i.e. confined to the spectral band of the VIS channel of the current generation of Meteosat satellite) with an algorithm accounting for water vapour and ozone absorption, aerosol scattering and surface anisotropy. The algorithm has been applied to one year (1996) of Meteosat data in order to document the seasonal variations of the surface albedo. The analysis of these results also revealed a potential influence of intense biomass burning activities on the observed seasonal surface albedo changes at a continental scale over Africa (Pinty et al, 2000c). Thus the algorithm could also contribute to the monitoring of biomass burning. It is expected that the spectral information from MSG will provide a better product since better corrections for aerosol will be possible.

4. GERB

The Geostationary Earth Radiation Budget Experiment (GERB) is a visible-infrared radiometer for Earth radiation budget studies (Harries, 2000). It makes accurate measurements of the shortwave (SW) and longwave (LW) components of the radiation budget at the top of the atmosphere. It is the first ERB experiment from geostationary orbit. It measures the solar waveband from 0.32 – 4 μm and the total from 0.32 – 30 μm. The LW from 4 – 30 μm is obtained through subtraction. With a nominal pixel size of about 45 by 40 km (NS x EW) at nadir view it obtains an absolute accuracy better than 2.4 $Wm^{-2}ster^{-1}$ (< 1%) in the SW and better 0.4 $Wm^{-2}ster^{-1}$ for the SW. The channel co-registration with respect to SEVIRI is 3 km at the subsatellite point. The cycle time for full disk is 5 minutes for both channels (15 minutes for full radiometric performance). The derivation of products from GERB is described by Dewitte et al. (2000).

5. CONCLUDING REMARK

The Meteosat Second Generation (MSG) system will significantly enhance the observation capabilities for rapidly changing phenomena such as cloud and water vapour structures. These will help nowcasting, short range forecasting and numerical weather prediction through improved and more frequent products. The capabilities of MSG are also expected to be of great value to research in various disciplines. Notably investigations of convective phenomena could benefit from the operational 15 minute repeat cycle. The current network of Satellite Application Facilities provides the basis for a wide use of the capabilities of MSG for various disciplines in meteorology. Research is also expected to benefit from MSG observations as exemplified by the good response to the MSG Research Announcement of Opportunity (Govaerts et al., 2000b and ESA, 2000).

More information on MSG is available on the EUMETSAT webpage under www.eumetsat.de.

6. REFERENCES

Eyre, J., Brownscombe, J. L., Allam, R. J., 1984: Detection of fog at night using Advanced Very High Resolution Radiometer (AVHRR) imagery. Meteorological Magazine, 113, 1984.

Dewitte, S., N. Clerbaux, L. Gonzalez, A. Hermans, A. Ipe, A. Joukoff and G. Sadowski, 2000: Generation of GERB unfiltered radiances and fluxes. Proceedings of the 2000 EUMETSAT Meteorological Satellite Data Users' Conference, Bologna, EUM-P29, p. 72 – 78.

ESA, 2000: First MSG RAO Workshop. Proceedings of the workshop in Bologna, Italy, 17 –19 May 2000, ESA SP-452, pp. 228.

EUMETSAT and SAI, 1999: Meteosat Second Generation Opportunities for Land Surface Applications. Report compiled by J. Cihlar, A. Belward and Y. Govaerts based on workshops held at EUMETSAT and the Space Applications Institute (SAI) of the Joint Research Centre at Ispra, EUM SP 01, pp. 67.

Govaerts, Y. A. Arriaga and J. Schmetz, 2000a: Operational vicarious calibration of the MSG/SEVIRI solar channels. To appear in Advances in Space Research.

Govaerts, Y., E. Oriol-Pibernat, J. Fischer and M. Menenti, 2000b: Overview of the first Metesat Second Generation Research Announcement of Opportunity Workshop. Proceedings of the 2000 EUMETSAT Meteorological Satellite Data Users' Conference, Bologna, EUM-P29, p. 99 – 105.

Hanson, C.G., M. Williams and L.C.J. van de Berg, 2000: 5-minute Meteosat imagery in support of the Mesoscale Alpine Programme. Proceedings of 'The 2000 EUMETSAT Meteorological Satellite Data Users' Conference', Bologna, Italy, 29 May – 2 June 2000, EUM P-29, p. 785 –796.

Harries, J.E., 2000: The Geostationary Earth radiation Budget experiment: Status and Science. Proceedings of the 2000 EUMETSAT Meteorological Satellite Data Users' Conference, Bologna, EUM-P29, p. 62 – 71.

Holmlund, K., 1998: The utilisation of statistical properties of satellite-derived atmospheric motion vectors to derive quality indicators. Wea. Forecasting, 13, 1093 –1104.

Holmlund, K., 1999: The use of Observations error as an extension to Barnes interpolation scheme to derive smooth instantaneous vector fields from satellite-derived Atmospheric Motion Vectors. Proceedings of the 1999 EUMETSAT Meteorological Satellite Data Users' Conference, Copenhagen, Denmark. EUM-P26. P633-637.

Holmlund, K., 2000: The Atmospheric Motion Vector Retrieval Scheme for Meteosat Second Generation.. Proceedings of the 5th International Winds Workshop, Lorne, Australia, EUM-P28, p. 201-208.

Lutz, H J, 1999: Cloud processing for Meteosat Second Generation. EUMETSAT Technical Department, Technical Memorandum No. 4, pp. 26.

Ma, X.L., T. Schmit and W.L. Smith, 1999: A non-linear retrieval algorithm – its application to the GOES-8/9 sounder. J. Appl. Meteorol., 38, 501 – 513.

Menzel, W.P., W.L.Smith and T.R. Stewart, 1983: Improved cloud motion wind vector and altitude assignment using VAS. Journal of Climate and Applied Meteorology, 22, 377-384.

Menzel, W.P., F.C. Holt, T.J. Schmit, R.M. Aune, A.J. Schreiner, G.S. Wade and D.G. Gray, 1998: Application of GOES-8/9 soundings to weather forecasting and nowcasting. Bull. Am. Meteor. Soc., 79, 2059 - 2077.

Munro, R., G. Kelly, M. Rohn and R. Saunders, 1998: Assimilation of Meteosat radiance data within the 4dvar system at ECMWF. Proceedings of the 4th International Winds Workshop, Saanenmöser, Switzerland, 20 – 23 October 1998, EUM Publication P 24, 299 – 306.

Levizzani, V., 1998: METEOSAT rapid scan during MAP-SOP. MAP Newsletter, No. 8.

Orsolini, Y.J. and F. Karcher, 2000: Total-ozone imaging over North America with GOES-8 infrared measurements. Q. J. R. Meteorol. Soc., 126,1557 – 1561.

Pili, P., 2000: Calibration of SEVIRI. Proceedings of 'The 2000 EUMETSAT Meteorological Satellite Data Users' Conference', Bologna, Italy, 29 May – 2 June 2000, EUM P-29, p. 33 – 39.

Pinty, B., Roveda, F., Verstraete, M.M., Gobron, N., Govaerts, Y., Martonchik, J.V., Diner, D.J., and Kahn, R.A. (2000a) Surface albedo retrieval from Meteosat: Part 1: Theory, Journal of Geophysical Research, Vol. 105, 18099-18112.

Pinty, B., Roveda, F., Verstraete, M.M., Gobron, N., Govaerts, Y., Martonchik, J.V., Diner, D.J., and Kahn, R.A. (2000b) Surface albedo retrieval from Meteosat: Part 2: Applications, JGR, Journal of Geophysical Research, Vol.105, 18113-18134.

Pinty, B., Verstraete, M.M., Gobron, N., Roveda, F., Govaerts, Y. (2000c) Do human-induced fires affect the Earth surface reflectance at continental scale?, EOS Transactions of the AGU, Vol. 81, 381-389.

Riishojgaard, L. P. On four-dimensional variational assimilation of ozone data in weather prediction models. Q. J. R. Meteorol. Soc., 122, 1545-1571, 1996.

Rodgers, C., 1976: Retrieval of atmospheric temperature and composition from remote measurements of thermal radiation. Rev. Geophys. And Space Physics.

Rosci, P., A. Balzamo, L. De Leonibus and F. Zauli, 2000: Improvements of automatic detection and extrapolation of convective phenomena using MAP rapid scan Meteosat images, Proceedings of 'The 2000 EUMETSAT

Meteorological Satellite Data Users' Conference', Bologna, Italy, 29 May – 2 June 2000, EUM P-29, p. 797 – 804.

Rosenfeld, D., and I.W. Lensky, 2000: Satellite-based insights into precipitation formation processes in continental and maritime clouds. Bull. American Meteorol. Soc., 79, 2457 –2476.

Saunders R.W. and K.T. Kriebel, 1988: An improved method for detecting clear sky and cloudy radiances from AVHRR data. Int. J. Remote Sensing, 9, 123-150.

Schmetz J., K. Holmlund, J. Hoffman, B. Strauss, B. Mason, V. Gaertner, A. Koch and L. van de Berg, 1993: Operational cloud motion winds from Meteosat infrared images, J. Appl. Met., 32, 1206-1225.

Schmetz, J., C. Geijo, W.P. Menzel, K. Strabala, L. van de Berg, K. Holmlund and S. Tjemkes, 1995: Satellite observations of upper tropospheric relative humidity, clouds and wind field divergence. Beitr. Phys. Atmosph., 68, 345 - 357.

Schmetz, J., K. Holmlund, H. P. Roesli and V. Levizzani, 2000: On the use of rapid scans. Proceedings of the 5th International Winds Workshop, 28 February – 3 March 2000, Lorne, Australia, EUM Publication EUM P-28, p. 227-234.

Szantai, A., F. Desalmand, M. Desbois and P. Lecomte, 2000: Tracking low-level clouds over Central Africa on Meteosat images. Proceedings of 'The 2000 EUMETSAT Meteorological Satellite Data Users' Conference', Bologna, Italy, 29 May – 2 June 2000, EUM P-29, p. 813 – 820.

Tjemkes, S.A. and J. Schmetz, 1997: Synthetic Satellite Radiances using the Radiance Sampling Method, J. Geophys. Res., Vol. 102(D2), 1807-1818.

Tjemkes, S. and P. Watts, 2000: Cloud properties from Meteosat. Proceedings of the 2000 EUMETSAT Meteorological Satellite Data Users' Conference, Bologna, EUM-P29, p. 314 – 317.

Velden, C. S., D. Stettner and J. Daniels, 2000: Wind vector fields derived from GOES rapid-scan imagery. Proceedings of the 10th Conference on Satellite Meteorology and Oceanography. 9 – 14 January 2000, Long Beach California, American Meteorological Society, p. 20 - 23.